



Designer Exosomes for Targeted Delivery of a Novel Therapeutic Cargo to Enhance Sorafenib-Mediated Ferroptosis in Hepatocellular Carcinoma

Xiaoju Li^{1†}, Qianqian Yu^{2†}, Runze Zhao^{1†}, Xinyan Guo¹, Chenlin Liu¹, Kuo Zhang¹, Wangqian Zhang¹, Jinghan Liu¹, Jinzheng Yu¹, Shuning Wang¹, Qiang Hao¹, Weina Li¹, Wei Zhang¹, Meng Li¹, Yingqi Zhang^{1*}, Cun Zhang^{1*} and Yuan Gao^{1*}

OPEN ACCESS

Edited by:

Yunfei Xu,
Shandong University, China

Reviewed by:

Qiang Wang,
Nanjing Drum Tower Hospital, China
Feng Zhang,
Nanjing University of Chinese
Medicine, China

*Correspondence:

Yuan Gao
gaoyuan321@fmmu.edu.cn
Cun Zhang
zhangcun@fmmu.edu.cn
Yingqi Zhang
zhangyqh@fmmu.edu.cn

[†]These authors have contributed
equally to this work

Specialty section:

This article was submitted to
Cancer Molecular Targets
and Therapeutics,
a section of the journal
Frontiers in Oncology

Received: 17 March 2022

Accepted: 24 May 2022

Published: 24 June 2022

Citation:

Li X, Yu Q, Zhao R, Guo X, Liu C,
Zhang K, Zhang W, Liu J, Yu J,
Wang S, Hao Q, Li W, Zhang W, Li M,
Zhang Y, Zhang C and Gao Y (2022)
Designer Exosomes for Targeted
Delivery of a Novel
Therapeutic Cargo to Enhance
Sorafenib-Mediated Ferroptosis in
Hepatocellular Carcinoma.
Front. Oncol. 12:898156.
doi: 10.3389/fonc.2022.898156

¹ State Key Laboratory of Cancer Biology, Biotechnology Center, School of Pharmacy, The Fourth Military Medical University, Xi'an, China, ² Department of Oncology, Tongji Hospital, Tongji Medical College, Huazhong University of Science and Technology, Wuhan, China

Sorafenib is one of the few effective first-line drugs approved for the treatment of advanced hepatocellular carcinoma (HCC). However, the development of drug resistance is common among individuals with HCC. Recent evidence indicated that the anticancer activity of sorafenib mainly relies on the induction of ferroptosis. Furthermore, in our study, genes that suppress ferroptosis, especially GPX4 and DHODH, were enriched in sorafenib-resistant cells and primary tissues and were associated with poor prognosis of HCC patients who received sorafenib treatment. Therefore, a new ferroptosis inducer comprising a multiplex small interfering RNA (multi-siRNA) capable of simultaneously silencing GPX4 and DHODH was created. Then, exosomes with high multi-siRNA loading and HCC-specific targeting were established by fusing the SP94 peptide and the N-terminal RNA recognition motif (RRM) of U1-A with the exosomal membrane protein Lamp2b. The results from the *in vitro* and *in vivo* experiments indicate that this tumor-targeting nano-delivery system (Exo^{SP94-lamp2b-RRM}_multi-siRNA) could enhance sorafenib-induced ferroptosis and overcome sorafenib resistance. Taken together, HCC-targeted exosomes (Exo^{SP94-Lamp2b-RRM}) could specifically deliver multi-siRNA to HCC tissues, enhance sorafenib-induced ferroptosis by silencing GPX4 and DHODH expression and consequently increase HCC sensitivity to sorafenib, which opens a new avenue for clinically overcoming sorafenib resistance from the perspective of ferroptosis.

Keywords: hepatocellular carcinoma, resistance, sorafenib, engineered exosome, ferroptosis

INTRODUCTION

Hepatocellular carcinoma (HCC) was ranked as the sixth most commonly diagnosed cancer and the fourth leading cause of cancer-related death worldwide in 2018 (1, 2). In the early stages of HCC, curative treatment can be achieved with tumor ablation, resection, or liver transplantation (3). However, the majority of HCC patients are already in the middle or late stages at the time of

diagnosis, missing the optimal window for curative treatment. Sorafenib is the first systemic therapy shown to improve survival in HCC and has been approved by the U.S. Food and Drug Administration (FDA) for treatment of unresectable HCC (4). Despite their initial response, sorafenib-treated tumors rarely regress completely, and most patients develop disease progression. Therefore, to improve the survival and quality of life of patients with HCC, combination therapies should be considered as a potentially superior treatment option.

Ferroptosis is a recently discovered form of programmed cell death characterized by iron-dependent accumulation of lipid peroxides to lethal amounts (5). A growing amount of evidence indicates that ferroptosis can be induced by inhibiting cystine/glutamate transporter (system x_c^-) activity, downregulating GPX4 or DHODH expression, and accumulating reactive oxygen species (ROS) (6). Recent reports have shown that sorafenib can induce ferroptosis by inhibiting system x_c^- (7). Moreover, numerous studies suggest that the anticancer activity of sorafenib mainly relies on inducing ferroptosis (5, 8–11). Therefore, targeting constituents of ferroptosis might be a promising strategy to increase sorafenib efficacy and overcome sorafenib resistance.

Herein, we first found that ferroptosis suppressor genes, especially GPX4 and DHODH, are enriched in sorafenib-resistant cells and primary tissues from patients and are associated with poor prognosis of HCC patients who receive sorafenib treatment. Then, we created a novel ferroptosis inducer comprising a multiplex small interfering RNA (multi-siRNA) suitable for simultaneously silencing GPX4 and DHODH. Then, exosomes (Exo^{SP94-lamp2b-RRM}) with high tumor targeting ability and high multi-siRNA loading efficacy were constructed to deliver the multi-siRNA cargo. Using *in vitro* and *in vivo* models, we demonstrated that this tumor-targeting nanodrug (Exo^{SP94-lamp2b-RRM}-multi-siRNA) could enhance sorafenib-induced ferroptosis and overcome sorafenib resistance, suggesting that it is a promising therapeutic strategy for treating sorafenib-resistant HCC.

MATERIALS AND METHODS

Antibodies and Inhibitors

The antibodies used targeted the following proteins (dilutions used are included):

GAPDH (CW0101: immunoblotting, 1:1000) from CWBIOTECH; F-actin (40734ES75: immunofluorescence, 1:100) from YEASEN; U1A (10212: immunoblotting, 1:500) from Proteintech; CD63 (67605-1-Ig: immunoblotting, 1:5000) from Proteintech; CD9 (60232-1-Ig: immunoblotting, 1:5000) from Proteintech; TSG101 (14497-1-AP: immunoblotting, 1:1000) from Proteintech; GPX4 (67763-1-Ig: immunoblotting, 1:5000; IHC, 1:1000) from Proteintech; and DHODH (14877-1-AP: immunoblotting, 1:2000; IHC, 1:100) from Proteintech.

The inhibitors used are as follows:

Sorafenib (HY-10201: 10 μ M for the *in vitro* assay and 30 mg/kg for the *in vivo* assay) and Ferrostatin-1 (HY-100579: 60 nM

for the *in vitro* assay), and ferrostatin-1 (HY-100579: 5 mg/kg, intraperitoneal injection for the *in vivo* assay) were obtained from MedChem Express.

Cell Lines and Culture

The HepG-2 and HEK-293T cell lines were obtained from the Type Culture Collection of the Chinese Academy of Sciences (Shanghai, China). These cell lines were authenticated by the analysis of short tandem repeat (STR) profiles, and all of them matched those of the standard cell lines in the DSMZ data bank. These cells tested negative for cross-contamination of other human cells and mycoplasma contamination. The sorafenib-resistant HepG-2 cell line (HepG-2R) was generated by continuous treatment of HepG2 cells with sorafenib up to 10 μ M and maintained as previously described (12). HepG-2, HepG-2R and HEK-293T cells were cultured in DMEM containing 10% fetal bovine serum and 1% penicillin-streptomycin.

Plasmid Construction

Briefly, the sequences for SP94 peptide (SFSIIHTPILPL), the CDS sequences of Lamp2b and the CDS sequences of the N-terminal RNA recognition motif (RRM) of U1-A were orderly arranged from N-terminal to C-terminal. Then the sequence encoding the above fusion protein was digested with BamHI-XhoI and cloned into pcDNA3.1(+) vector. The clones were confirmed by DNA sequencing and stored for the following experiments.

Exosome Purification

For exosome isolation from HEK-293T cells, cells were transfected with control or SP94-Lamp2b-RRM expressing plasmids with Lipofectamine3000. 12 h later, cells were further cultured in DMEM with 10% exosome-depleted FBS (ultracentrifugation at 120,000 \times g for 16 h) for 24–36 h. Then, the culture medium was precleared by centrifugation at 500 \times g for 15 min and then at 10000 \times g for 20 min. Exosomes were isolated by ultracentrifugation at 110000 \times g for 70 min at 4°C and washed in PBS using the same centrifugation conditions. The concentration of exosomes was determined by measuring total exosomal protein using a Pierce BCA Protein Assay Kit (Thermo Scientific, USA) according to the manufacturer's instructions. NanoSight and transmission electron microscopy were used to determine the size distribution, concentration and morphology of the exosomes. For siRNA loading experiments, 100 nM corresponding siRNAs were transfected with Lipofectamine 3000. Twenty-four hours later, the cells were further cultured in DMEM with 10% exosome-depleted FBS for another 24 h, followed by exosome isolation.

Transmission Electron Microscope Assay

Cells were collected and fixed with 2.5% glutaraldehyde. Subsequently, cells were postfixated in 2% tetroxide and dehydrated through a series of gradient ethanol solutions. Samples were embedded in epoxy resin, cut into thin slices, and placed onto a nickel grid. Images were acquired using a Tecnai G2 Spirit transmission electron microscope (Thermo Fisher).

Intracellular ROS Measurements

A lipid ROS assay was performed as described previously. Briefly, cells were incubated with PBS containing 10 μ M DCFDA dye in a cell culture incubator for 30 min. Cells were then collected and washed twice with PBS followed by resuspension in 200 μ l of PBS. ROS levels were analyzed using a Beckman CytoFLEX system through the FITC channel.

Detection of Malondialdehyde (MDA)

Analysis of lipid peroxidation was assessed by quantifying the MDA concentration in cell lysates using a Lipid Peroxidation MDA Assay Kit (S0131, Beyotime) in accordance with the manufacturer's instructions.

Animal Study

Six-week-old, male, athymic BALB/c nude mice were used. All animal experiments were carried out under protocols approved by the Animal Care and Use Committee of Fourth Military Medical University.

For *in vivo* tracking of exosomes, purified exosomes with the indicated modifications were labeled with the fluorescent dye DiR at a final concentration of 8 μ M (Invitrogen). Labeled exosomes were collected by ultracentrifugation after washing with saline and stored in saline before use. Mice were injected with labeled exosomes (100 μ g at the protein level in 100 μ L) *via* tail vein injection. Mice were subjected to fluorescent living imaging 6 h after injection with an *in vivo* imaging system (IVIS lumina II).

For orthotopic implantation, six-week-old male nude mice were anesthetized with 3% (w/v) pentobarbital sodium by intraperitoneal injection. Then, 2×10^6 sorafenib-resistant HepG-2 cells stably expressing luciferase were surgically implanted into the left liver lobes of mice. Tumor growth was monitored by bioluminescence with an *in vivo* imaging system (IVIS lumina II). Two weeks after inoculation, mice were randomized to each group and began to receive different treatments. In the sorafenib treatment group, sorafenib (30 mg/kg) was given every 3 days. In the sorafenib and exosome combination treatment group, sorafenib was administered at the same dose, and 100 μ g of the indicated exosomes (at the protein level) was injected *via* the tail vein 24 h after every sorafenib administration. At the end of the experiment, mice were sacrificed. Tumor bearing liver tissues and the main organs were collected for the following experiments.

Immunohistochemistry

This experiment was performed as previously described (13). Briefly, sections (4 μ m thick) of paraffin-embedded samples were deparaffinized and rehydrated in a graded series of ethanol. After inactivation of endogenous peroxidase activity with 3% H_2O_2 in methanol for 10 min, the sections were washed three times in PBS and blocked with goat serum for 20 min. Then, they were incubated with primary antibodies in a humid container at 4°C overnight. After the addition of the PowerVision™ complex, tissue sections were incubated at 37°C for 20 min followed by

treatment with DAB. PBS in place of primary antibody was used as a negative control.

Statistical Analysis

The data are presented as the mean \pm s.e.m. from at least three independent experiments. Statistical analysis was performed using GraphPad Prism software. A random number table was used to randomize the mice into control and treatment groups. The numbers of mice were determined on the basis of our pretests and previous experience with similar experiments. A value of $P < 0.05$ was considered statistically significant. The statistical tests were two-sided.

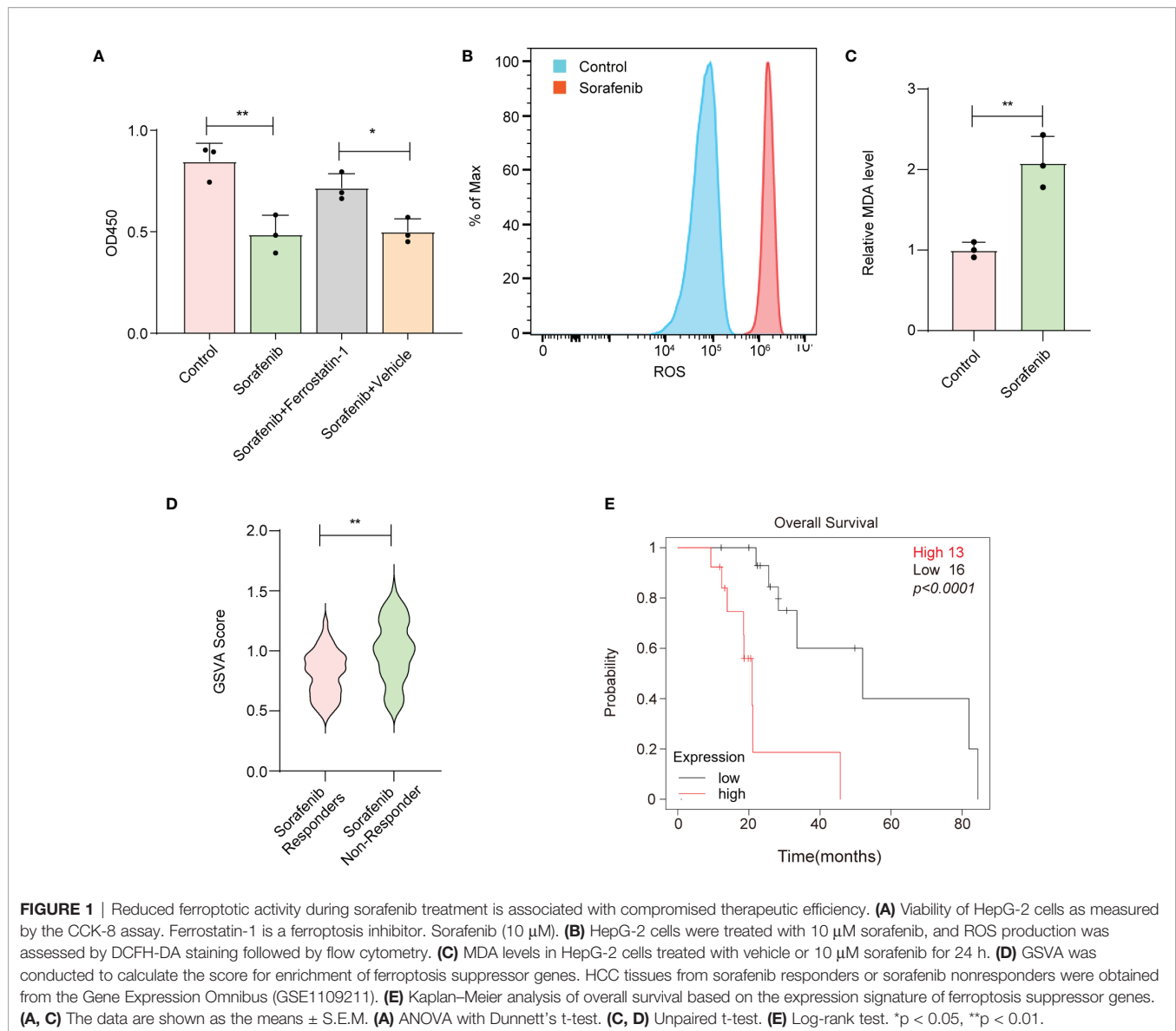
RESULTS

Suppressed Ferroptotic Activity During Sorafenib Treatment Is Associated With Compromised Therapeutic Efficiency

To confirm whether sorafenib could induce ferroptosis in HCC cells, we performed a CCK-8 assay. Our data showed that sorafenib-mediated cell death in the human HCC cell line HepG-2 was blocked by ferrostatin-1 (a ferroptosis inhibitor) (Figure 1A, Figure S1A). The accumulation of reactive oxygen species (ROS) and lipid peroxidation are key events in ferroptosis (14); thus, we analyzed the levels of ROS and the end products of lipid peroxidation (i.e., MDA) in HepG-2 cells. The results indicated that sorafenib increased the levels of ROS and MDA in HepG-2 cells (Figures 1B, C). Apart from ferroptosis-suppressing agents, numerous genes have been identified as key ferroptosis suppressors. For example, glutathione peroxidase 4 (*GPX4*) resides in the center of a network that functions to prevent the accumulation of lipid hydroperoxides, thereby strongly suppressing ferroptosis (15). Interestingly, we constructed a ferroptosis suppressor gene signature and discovered that ferroptosis suppressor genes were enriched in sorafenib-resistant cells and primary tissues from HCC patients (Figure 1D, Figure S1B). Moreover, the results indicated that the high expression level of the ferroptosis suppressor gene signature was associated with poor prognosis of HCC patients who received sorafenib treatment (Figure 1E, Figure S1C). Therefore, the results suggest that suppressed ferroptotic activity is associated with sorafenib resistance.

Gene-Silencing Activities of the Multi-siRNA Against *GPX4* and *DHODH*

The above data suggest that silencing key ferroptosis suppressor genes increases the therapeutic effect of sorafenib. Among the ferroptosis suppressor genes, *GPX4* and *DHODH* can directly remove the dangerous products of iron-dependent lipid peroxidation and consequently protect the cell membrane from damage; when *GPX4* and *DHODH* expression and/or function are dysregulated, ferroptosis ensues (16, 17). Moreover, we found that the expression of *GPX4* and *DHODH* was upregulated in sorafenib-resistant patients (Figures 2A, B) and associated with



poor prognosis of HCC patients who received sorafenib treatment (Figures 2C, D). Meanwhile, GPX4 and DHODH expression was upregulated in sorafenib-resistant HCC cell line (HepG-2R) (Figure 2E). In light of these findings, we sought to interfere with the expression and function of these two genes at the same time. First, siRNAs targeting the human *GPX4* gene and human *DHODH* gene were designed and screened to determine their effectiveness. As shown in Figures 2F, G and Figures S2A, B, si-GPX4#1 and si-DHODH#1 were the most effective siRNAs in knocking down their respective proteins. Then, we designed a multi-siRNA containing the sequences corresponding to si-GPX4#1 and si-DHODH#1; the sequence “AUUGCAC” was used as a linker to connect si-GPX4#1 to si-DHODH#1. The results showed that this multi-siRNA could simultaneously suppress GPX4 and DHODH expression (Figure 2H).

Preparation and Characterization of SP94-Lamp2b-RRM Fusion Protein-Engineered Exosomes

Exosomes have been considered a good siRNA delivery vehicle to reduce drug resistance (18). However, low cargo encapsulation efficiency and the lack of cell-type specific targeting remain major hurdles for their potential clinical application. Recently, some RNA-binding proteins have been shown to significantly promote exosomal miRNA cargo loading *via* interaction with common short sequence motifs present in miRNAs (19). Therefore, we hypothesized that fusion of specific RNA-binding proteins with the exosomal membrane proteins can increase the loading efficiency of the desired RNAs. We fused the N-terminal RNA recognition motif (RRM) of U1-A with the C-terminus of Lamp2b (exosomal

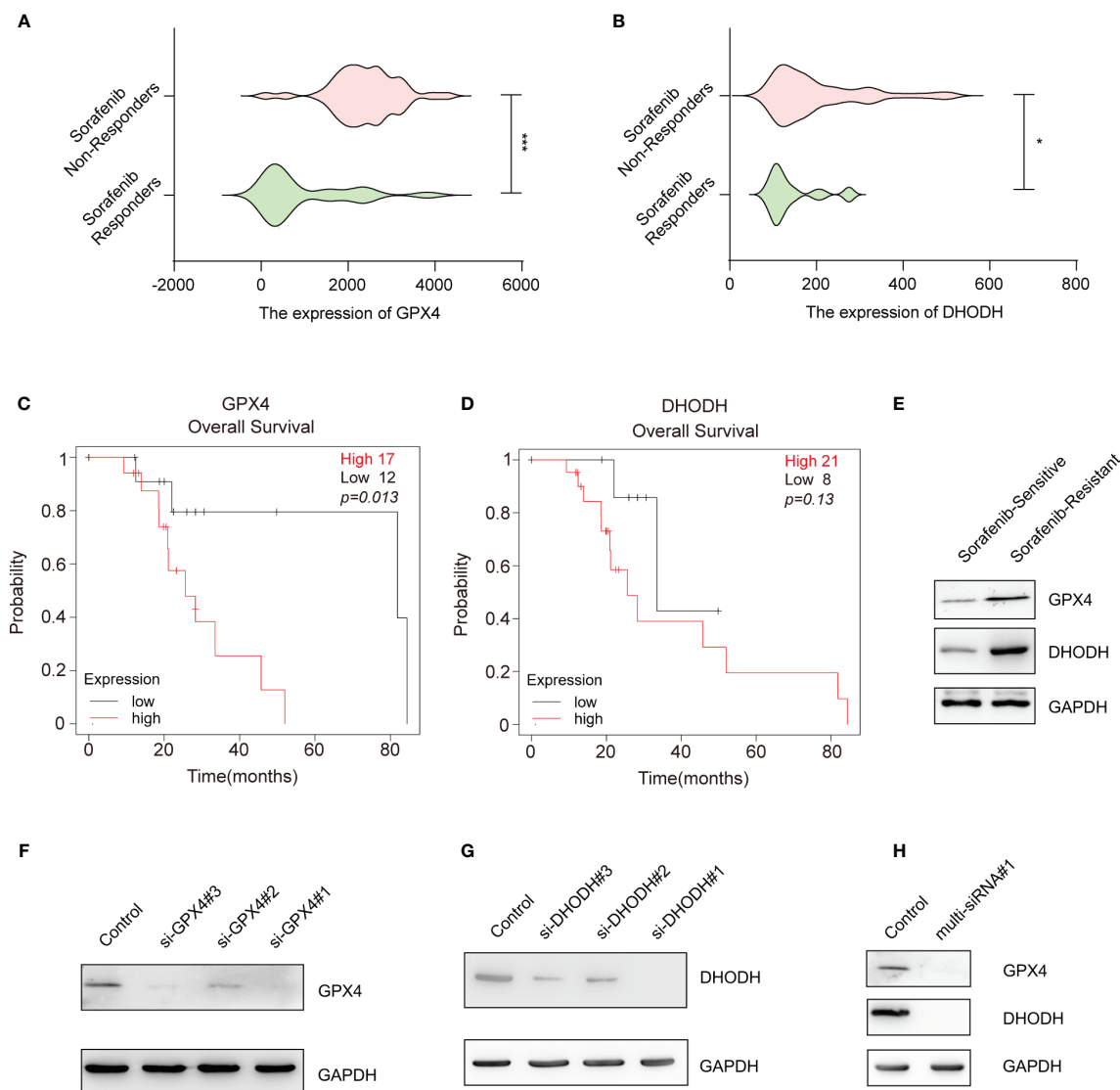
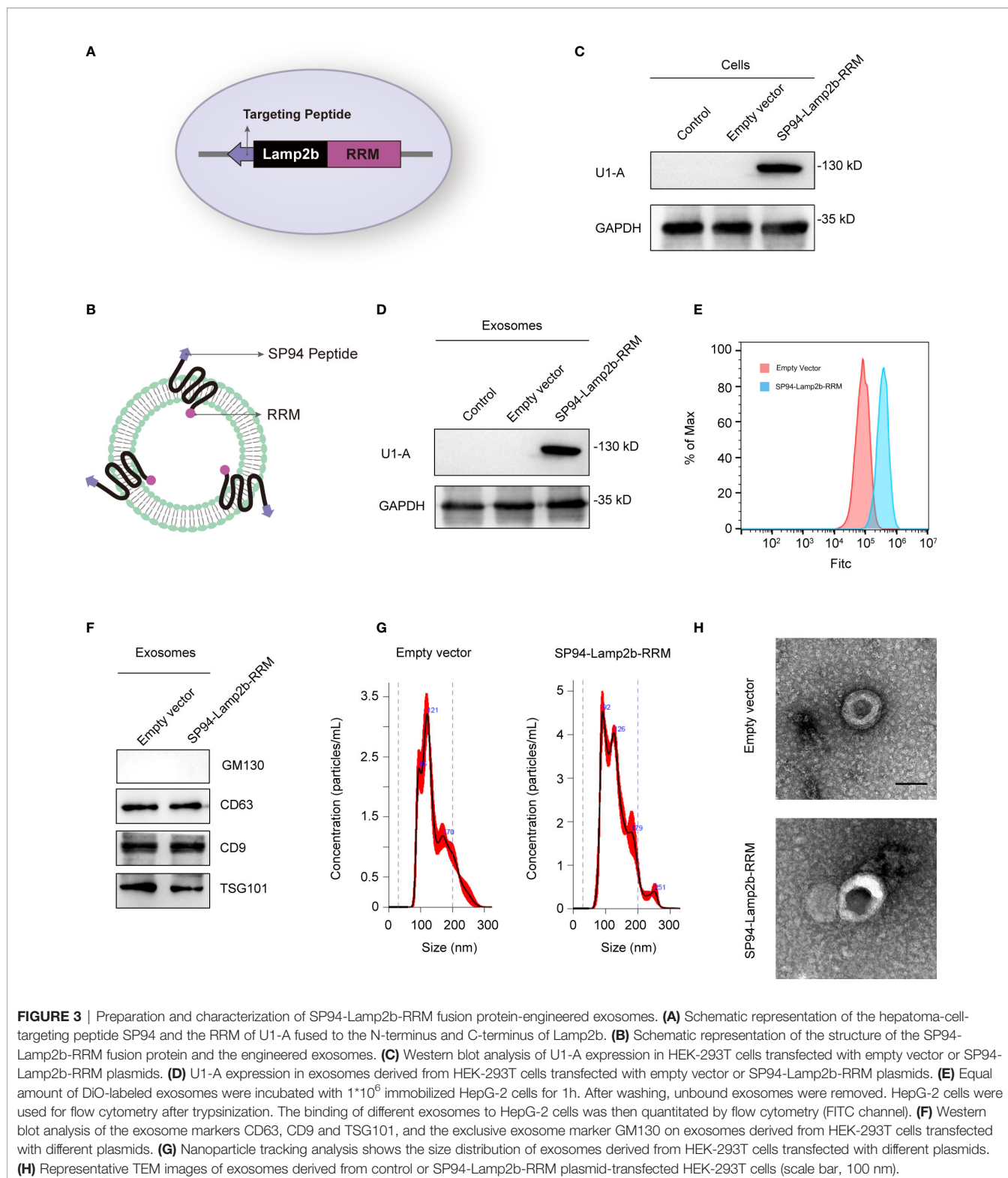


FIGURE 2 | Gene-silencing activities of multi-siRNA against GPX4 and DHODH genes. **(A)** GPX4 expression in HCC tissues from sorafenib responders ($n=21$) or sorafenib nonresponders ($n=43$) (gse109211). **(B)** That of DHODH in the HCC tissues of sorafenib responders ($n=21$) or sorafenib nonresponders ($n=43$) (gse109211). **(C)** Kaplan–Meier overall survival analysis of the GPX4 gene in HCC patients who received sorafenib treatment. **(D)** Kaplan–Meier overall survival analysis of the DHODH gene in HCC patients who received sorafenib treatment. **(E)** Western blotting for assessment of the protein levels of DHODH and GPX4 in sorafenib-sensitive HepG-2 or sorafenib-resistant HepG-2 (HepG-2R) cells. **(F)** Western blotting was conducted to detect GPX4 expression in HepG-2R cells transfected with scramble or GPX4 siRNAs. **(G)** Western blotting was conducted to detect DHODH expression in HepG-2R cells transfected with scramble or DHODH siRNAs. **(H)** HepG-2R cells were transfected with scramble siRNA or multi-siRNA#1 containing the si-GPX4#1 and si-DHODH#1 target sequences, and Western blotting was conducted to detect GPX4 and DHODH expression. **(A, B)** Unpaired *t*-test. **(C, D)** Log-rank test. * $p < 0.05$, *** $p < 0.001$.

surface protein) (**Figures 3A, B**). U1-A can bind the highly conserved sequence “AUUGCAC” in RNA *via* its N-terminal RRM (20). SP94 (protein sequence, SFSIIHTPILPL), is a novel peptide that has been reported to specifically bind to HCC cells (21). Therefore, we fused SP94 with the N-terminus of Lamp2b to enhance the tumor-targeting ability of the engineered exosomes (**Figures 3A, B**). The recombinant vector produced abundant expression of the fusion protein in transfected cells

(**Figure 3C**). As the engineered SP94-Lamp2b-RRM fusion protein could express on exosomes (**Figure 3D**), we analyzed the binding ability of these exosomes to HCC cells. The results showed that exosomes derived from HEK-293T cells transfected with SP94-Lamp2b-RRM could bind strongly to HCC cells (**Figure 3E**), indicating that the SP94-Lamp2b-RRM fusion protein was incorporated into exosomes. In addition, specific exosome markers (CD63, TSG101 and CD9) were



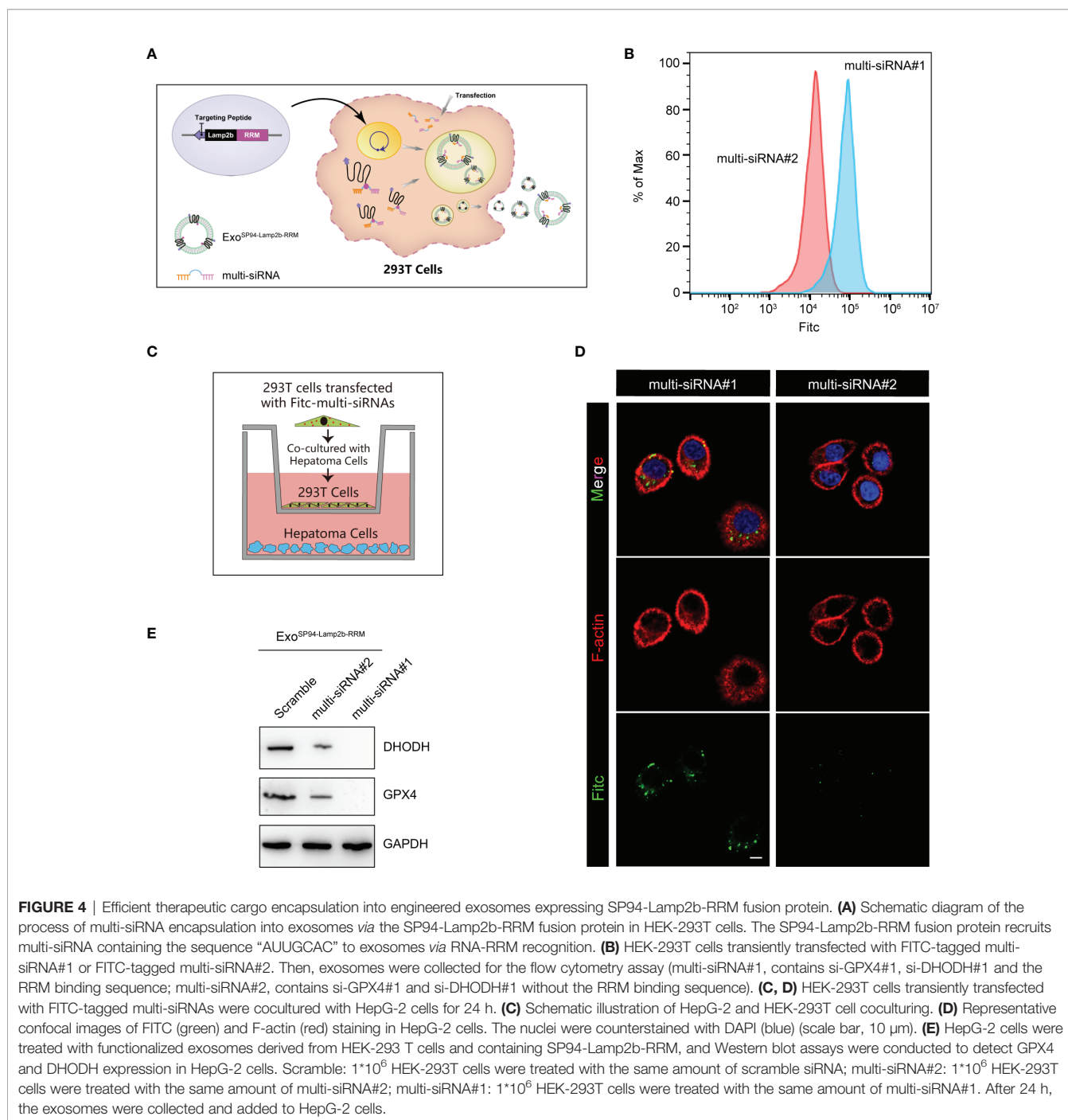
detected in the purified samples, while the Golgi marker GM130 was barely detectable (**Figure 3F**). Nanoparticle tracking analysis (NTA) revealed that the exosomes were similar in number and had a similar size distribution between

the groups (**Figure 3G**). Transmission electron microscopy (TEM) confirmed that the purified exosomes exhibited a typical round-shaped vesicular morphology and were within the appropriate size range (**Figure 3H**).

Efficient Therapeutic Cargo Encapsulation Into SP94-Lamp2b-RRM Fusion-Protein-Engineered Exosomes

Next, we explored whether the engineered SP94-Lamp2b-RRM fusion protein could promote RNA loading during exosome biogenesis. First, HEK-293T cells overexpressing the SP94-Lamp2b-RRM fusion protein were transfected with 100 nM corresponding FITC-tagged multi-siRNA (**Figure 4A**). Then,

an equal number of exosomes from each group was evaluated by flow cytometry. The results showed that a higher amount of multi-siRNA containing the RRM recognition motif “AUUGCAC” could be sorted into exosomes compared to that of multi-siRNA#2 without the RRM binding sequence (**Figure 4B**). HEK-293T cells were then cocultured with HepG-2 cells (**Figure 4C**). Images from the confocal microscope showed a higher level of multi-siRNA containing the RRM “AUUGCAC” in HepG-2 cells (**Figure 4D**). Consistent



with this finding, exosomes derived from HEK-293T cells transfected with the multi-siRNA containing the “AUUGCAC” sequence could significantly suppress the expression of GPX4 and DHODH in HCC cells (Figure 4E). These results suggest that the SP94-Lamp2b-RRM fusion protein promotes the exosomal loading of the “AUUGCAC” sequence linked to the multi-siRNA *via* RNA-protein interactions.

SP94-Lamp2b-RRM-Functionalized Exosomes Could Overcome Sorafenib Resistance by Enhancing Sorafenib-Induced Ferroptosis in HCC Cells

To investigate whether Exo^{SP94-Lamp2b-RRM} can bind to HCC cells, blank exosomes or Exo^{SP94-Lamp2b-RRM} were labeled with DiO and added to sorafenib-resistant HepG-2 cell cultures. Confocal assay showed that green fluorescence appeared within 15 min and intensified over time (up to 60 min) in the SP94-Lamp2b-RRM-functionalized exosomes treated group. By contrast, relatively low level of green fluorescence was observed in control exosomes treated cells up to 60 min, confirming the targeting ability of SP94-Lamp2b-RRM-functionalized exosomes to HCC cells (Figures 5A, B). Then, we treated sorafenib-resistant HepG-2 cells with exosomes (Exo^{SP94-Lamp2b-RRM}-multi-siRNA#1). The results showed that Exo^{SP94-Lamp2b-RRM}-multi-siRNA#1 could significantly enhance the effect of sorafenib (Figure 5C). Then, we further measured ROS and lipid peroxidation levels, which are the primary drivers of ferroptosis. The results showed that treatment with Exo^{SP94-Lamp2b-RRM}-multi-siRNA#1 significantly increased ROS and MDA levels in sorafenib-resistant cells (Figures 5D, E). In addition to biochemical analyses, TEM was used to observe morphological changes. Exo^{SP94-Lamp2b-RRM}-multi-siRNA#1-treated cells displayed diminished or vanished mitochondrial cristae and condensed mitochondrial membrane densities compared to Exo^{SP94-Lamp2b-RRM}-scramble-treated cells (Figure 5F). Moreover, we also found that Exo^{SP94-Lamp2b-RRM}-multi-siRNA#1 could enhance sorafenib-induced ferroptotic cell death (Figure 5G). Taken together, these results suggested that Exo^{SP94-Lamp2b-RRM}-multi-siRNA#1 could enhance sorafenib-induced ferroptosis in HCC cells by silencing the expression of GPX4 and DHODH.

SP94-Lamp2b-RRM-Functionalized Exosomes Could Efficiently Target Hepatocellular Carcinoma *In Vivo*

To confirm whether SP94-Lamp2b-RRM-functionalized exosomes could target HCC *in vivo*, we tracked the distribution of DiR-labeled exosomes. First, we established an orthotopic liver injection model and observed that SP94-Lamp2b-RRM-functionalized exosomes were mainly distributed to the liver (Figures 6A–C). Meanwhile, SP94-Lamp2b-RRM-functionalized exosomes could target HCC (Figures 6A–C). Next, sorafenib-resistant HepG-2 cells were subcutaneously inoculated into the left backs of mice. In the subcutaneous HCC model, we found that SP94-Lamp2b-RRM-functionalized exosomes were mainly distributed in the liver and

subcutaneous tumor tissues (Figure 6D, Figure S3A). The results from the different HCC models suggest that the SP94 targeting peptide dramatically enhances the ability of exosomes to bind HCC cells and tissues.

Therapeutic Effects of Cotreatment With SP94-Lamp2b-RRM-Functionalized Exosomes and Sorafenib in an HCC Mouse Model

Next, we explored the therapeutic effect of SP94-Lamp2b-RRM-functionalized exosomes combined with sorafenib *in vivo*. While the tumors of mice treated with sorafenib and Exo^{SP94-Lamp2b-RRM} containing scramble multi-siRNA grew rapidly, those of mice treated with sorafenib and Exo^{SP94-Lamp2b-RRM} containing multi-siRNA#1 were significantly reduced after 21 days of treatment (Figures 7A–C). However, the effect of sorafenib and Exo^{SP94-Lamp2b-RRM} containing multi-siRNA#1 on inhibiting tumor growth was diminished when cells were treated with the ferroptosis inhibitor ferrostatin-1 (Figures 7A–C). Similarly, mice from the sorafenib and Exo^{SP94-Lamp2b-RRM} containing multi-siRNA#1 cotreatment group had a longer life expectancy than did mice from the sorafenib and Exo^{SP94-Lamp2b-RRM} containing scramble multi-siRNA treatment group (Figure 7D). To examine the knockdown efficiency in each group, GPX4 and DHODH expression in primary tumor lesions was investigated by immunohistochemistry. The results showed that multi-siRNA#1 could significantly suppress GPX4 and DHODH expression *in vivo* (Figure 7E). Taken together, these results suggested that Exo^{SP94-Lamp2b-RRM}-multi-siRNA#1 could overcome sorafenib resistance *in vivo* by silencing the ferroptosis suppressor genes GPX4 and DHODH.

Systemic Toxicity Evaluation

To evaluate the systemic toxicity of Exo^{SP94-Lamp2b-RRM}, exosomes containing scramble or multi-siRNA#1 were injected into nude mice *via* tail vein. There was no significant difference in the body weights of mice in the two groups (Figure S4A). In addition, compared to the control group, the Exo^{SP94-Lamp2b-RRM} group showed relatively normal tissue structure and morphology (Figure 8). These results indicate that there was no obvious adverse effect after treatment with Exo^{SP94-Lamp2b-RRM}.

DISCUSSION

Our study demonstrated that sorafenib could induce ferroptosis in HCC cells, which is in line with the literature stating that the anticancer activity of sorafenib mainly relies on the induction of ferroptosis. What's more, we found that the expression of ferroptosis suppressor genes, especially GPX4 and DHODH, was enriched in sorafenib-resistant HCC cells and patient samples, which suggests that suppressed ferroptotic activity is associated with compromised therapeutic efficiency of sorafenib. Thus, precise elimination of ferroptosis suppressor genes might be a new promising strategy to enhance sorafenib efficacy and improve patient prognosis.

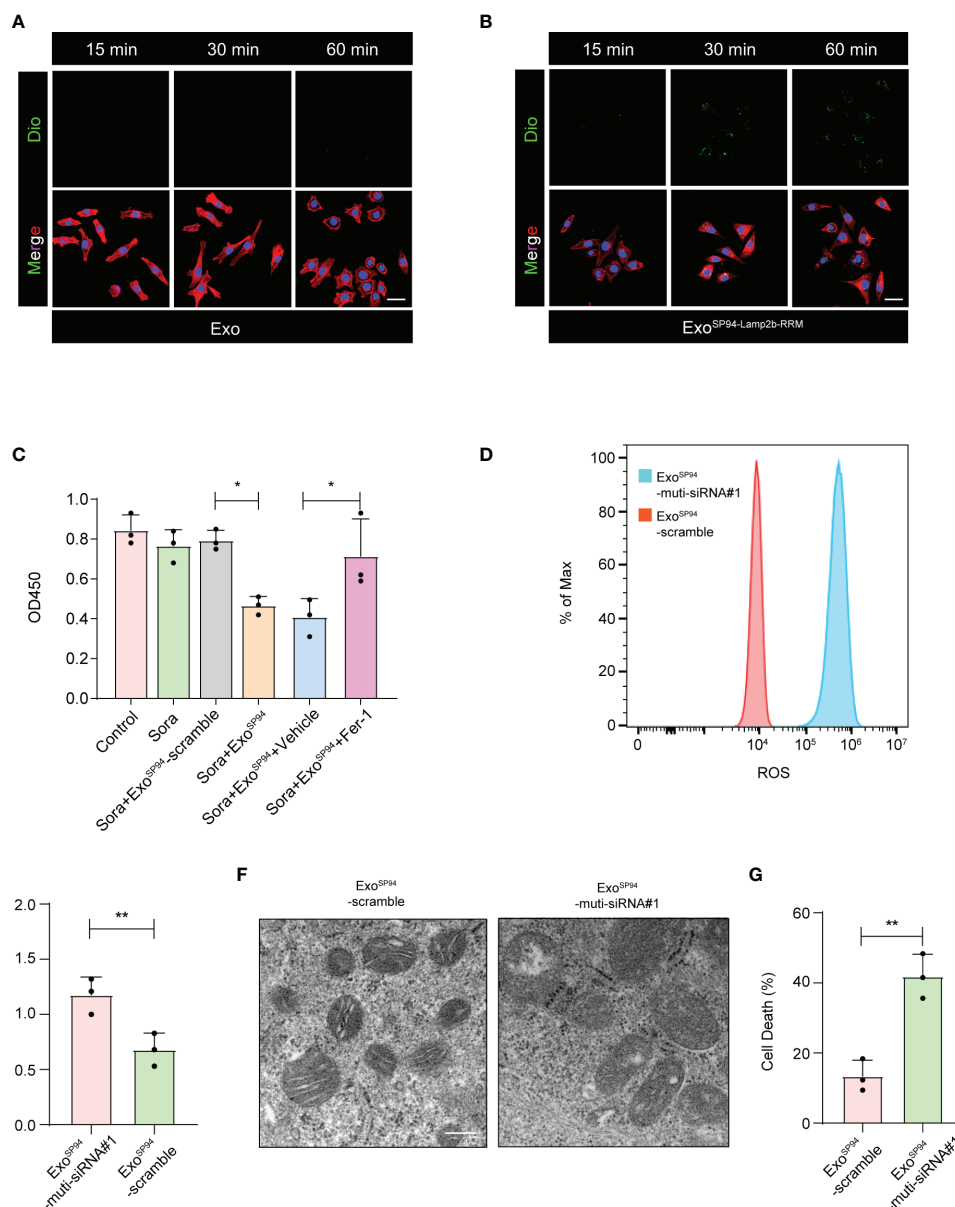


FIGURE 5 | SP94-Lamp2b-RRM-functionalized exosomes could overcome sorafenib resistance by enhancing sorafenib-induced ferroptosis in HCC cells. **(A–B)** Dio labeled engineered exosomes or control exosomes were incubated with HCC cells for 15, 30 or 60 min at 37°C. Then unbound exosomes were removed by PBS washing. Exosome endocytosis was analyzed by confocal microscopy. The nuclei and F-actin were counterstained with DAPI (blue) and TRITC phalloidin (red), respectively, (scale bar, 50 μ m). **(C)** Sorafenib-resistant HepG-2 cells treated with sorafenib and SP94-Lamp2b-RRM-functionalized exosomes containing scramble or multi-siRNA#1. Viability of sorafenib-resistant HepG-2 cells as measured by the CCK-8 assay. **(D)** Sorafenib-resistant HepG-2 cells were treated with sorafenib in combination with SP94-Lamp2b-RRM-functionalized exosomes containing scramble or multi-siRNA#1, and the ROS production was assessed by DCFH-DA staining followed by flow cytometry. **(E)** MDA levels of sorafenib-resistant HepG-2 cells treated with sorafenib and SP94-Lamp2b-RRM-functionalized exosomes containing scramble or multi-siRNA#1. **(F)** TEM images of mitochondria in sorafenib-resistant HepG-2 cells cotreated with sorafenib and SP94-Lamp2b-RRM-functionalized exosomes containing scramble or multi-siRNA#1. **(G)** Sorafenib-resistant HepG-2 cells were treated with sorafenib and SP94-Lamp2b-RRM-functionalized exosomes containing scramble or multi-siRNA#1. Cell death was determined by PI staining coupled with flow cytometry. **(C, E, G)** The data are shown as the means \pm S.E.M. **(C)** ANOVA with Dunnett's *t*-test. **(E, G)** Unpaired *t*-test. **p* < 0.05, ***p* < 0.01.

Ferroptosis is a form of regulated cell death that is induced by excessive lipid peroxide accumulation in cellular membranes (22–24). Cells have developed at least two major defensive arms to detoxify lipid peroxides: GPX4 and DHODH. Consequently,

disabling one arm forces cells to be more dependent on the other. For example, inhibition of either DHODH or GPX4 alone did not induce ferroptosis in HT-1080 cells, which is likely due to the relatively high endogenous expression of GPX4 and DHODH (25);

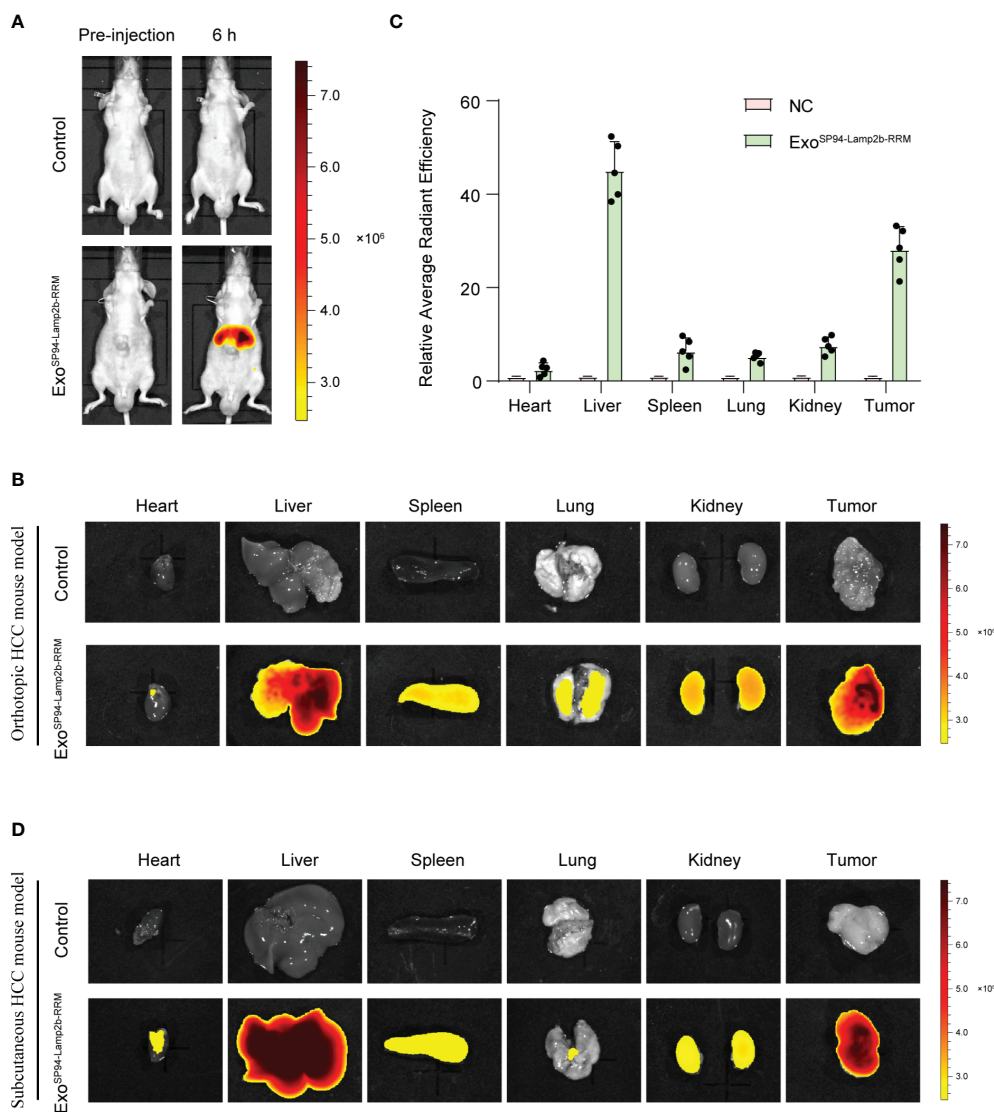


FIGURE 6 | SP94-Lamp2b-RRM-functionalized exosomes could efficiently target HCC *in vivo*. **(A–C)** Sorafenib-resistant HepG-2 cells were orthotopically inoculated into the left liver lobes of nude mice. SP94-Lamp2b-RRM-functionalized exosomes (100 μ g) were injected into nude mice *via* tail vein. **(A)** Mice were evaluated with a fluorescent live imaging system 6 h after injection. **(B)** Representative *ex vivo* fluorescence images of DiR-labeled exosomes in the main organs and HCC tissues. **(C)** Relative fluorescence intensity of DiR-labeled exosomes in different organs and liver cancer tissues. **(D)** Sorafenib-resistant HepG-2 cells were subcutaneously inoculated on the left backs of mice. SP94-Lamp2b-RRM-functionalized exosomes were loaded with DiR, and 100 μ g of exosomes was injected into mice *via* tail vein. Different organs and tumors were harvested to conduct fluorescence imaging. **(C)** The data are shown as the means \pm S.E. M; n=5.

interestingly, a GPX4 inhibitor combined with a DHODH inhibitor could synergistically suppress HT-1080 tumor growth. Similarly, in our study, the sorafenib-resistant cells and tissue samples exhibited high levels of GPX4 and DHODH expression. Therefore, disabling both arms might better enhance sorafenib-induced ferroptosis. Here, we created a multi-siRNA that can simultaneously knock down GPX4 and DHODH *in vitro* and *in vivo*. To our knowledge, this is the first ferroptosis inducer that can directly target two genes. Additionally, this novel construct provides a new approach for the clinical treatment of sorafenib-resistant cancer.

Because of their intrinsic nature, exosomes are biocompatible with the host immune system and have an innate ability to protect

and transport small RNAs and other critical molecules across biological barriers *in vivo*; they have been increasingly recognized as promising vehicles to deliver siRNA *in vivo* (26, 27). At present, the most common way to load nucleic acids into exosomes is *via* electroporation or direct encapsulation in donor cells (28); however, these methods have relatively low loading efficiencies. Meanwhile, *in vitro* loading of naked siRNAs into exosomes by electroporation could cause extensive siRNA aggregation and significantly reduce the level of bioactive siRNAs (29). Thus, there is an urgent need to develop a strategy for efficient loading of nucleic acids, especially siRNA. Recently, research conducted by our laboratory and others have observed that some RNA-binding

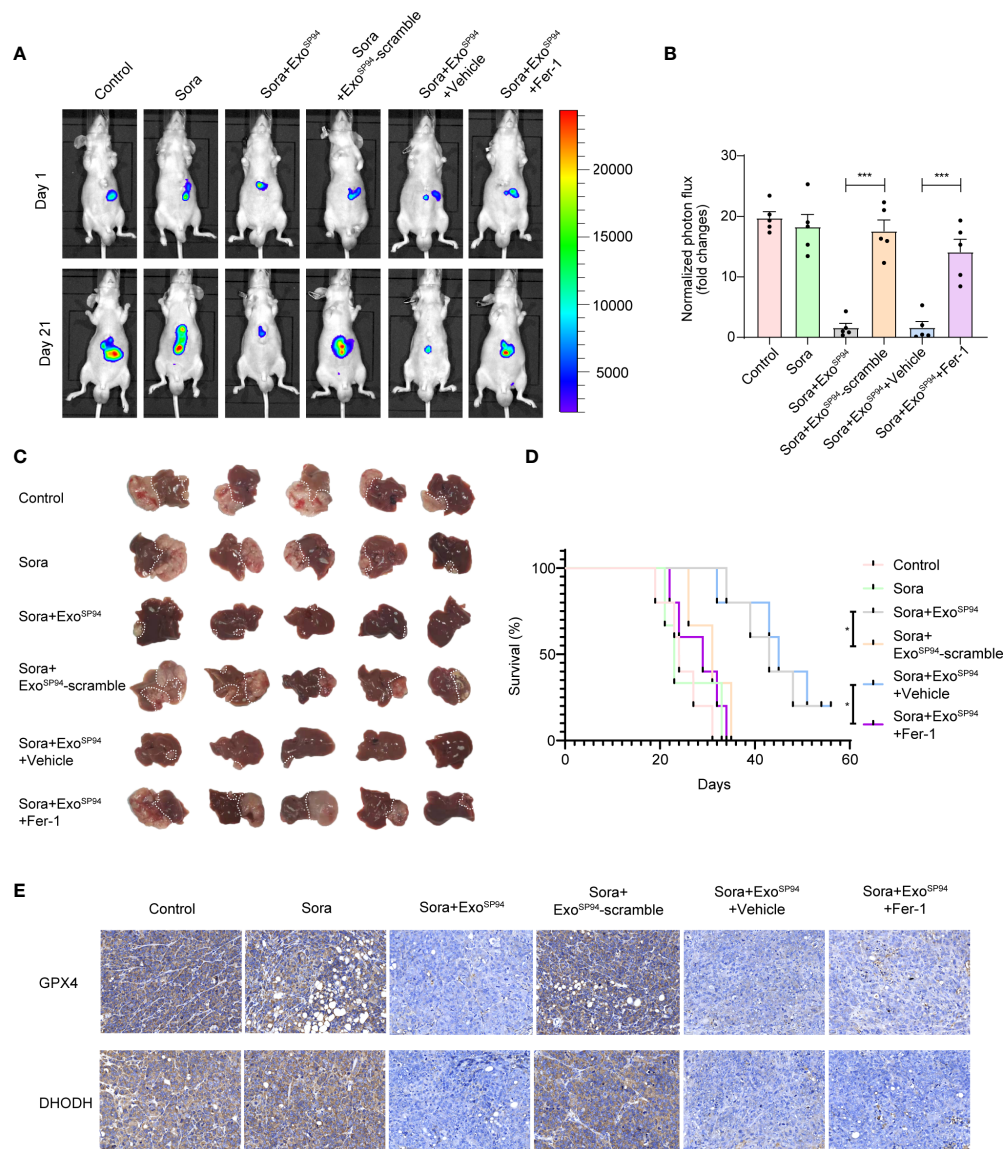
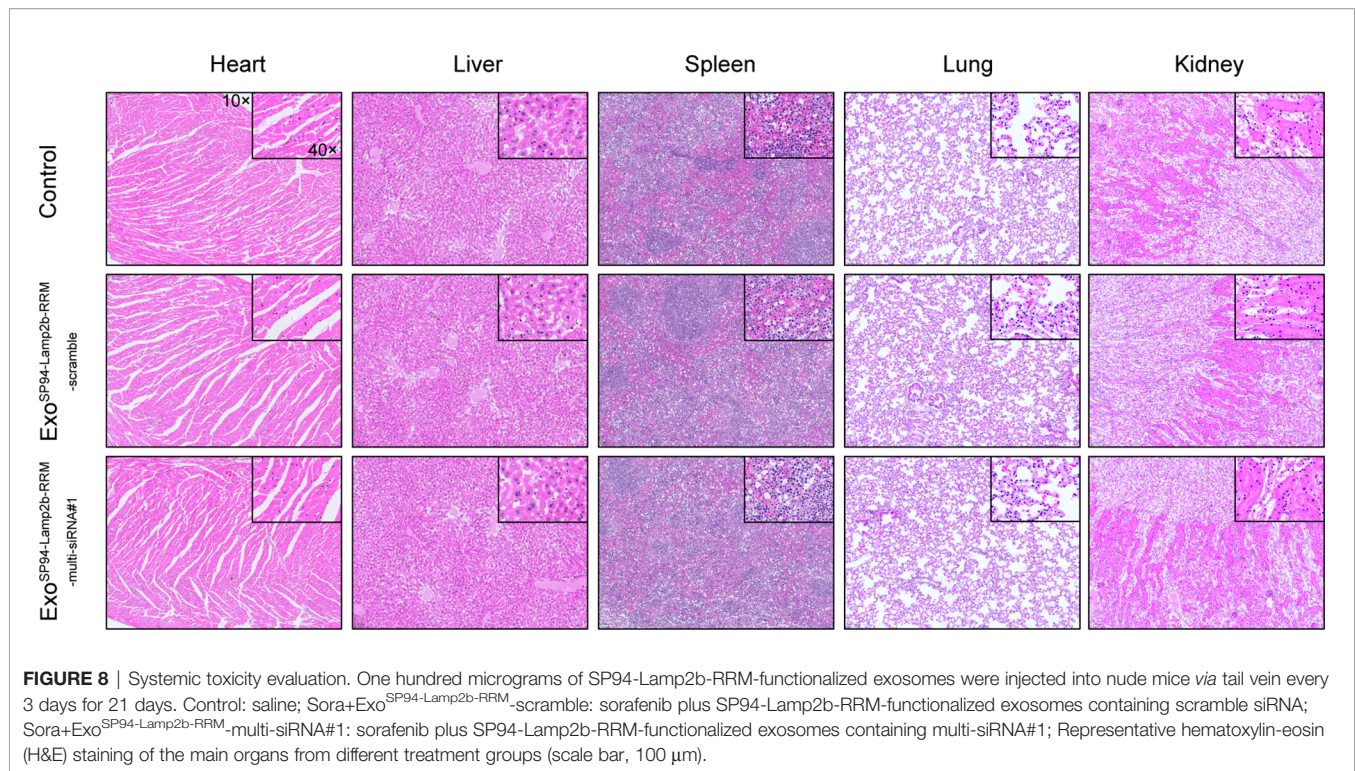


FIGURE 7 | Therapeutic effects of SP94-Lamp2b-RRM-functionalized exosomes and sorafenib in an HCC mouse model. Sorafenib-resistant HepG-2 cells were orthotopically injected into the left liver lobes of nude mice. Mice with a similar tumor size were used. Control: saline; Sora: sorafenib; Sora+Exo^{SP94}: sorafenib plus SP94-Lamp2b-RRM-functionalized exosomes containing multi-siRNA#1; Sora+Exo^{SP94}-scramble: sorafenib plus SP94-Lamp2b-RRM-functionalized exosomes containing scramble siRNA; Sora+Exo^{SP94}+Vehicle: sorafenib plus SP94-Lamp2b-RRM-functionalized exosomes containing multi-siRNA#1 in vehicle; Sora+Exo^{SP94}+Fer-1: sorafenib plus SP94-Lamp2b-RRM-functionalized exosomes in multi-siRNA#1 combined with ferostatin-1. Tumor growth was measured with an IVIS imaging system. **(A)** Representative tumor imaging on days 1 and 21 after the first treatment. **(B)** The normalized photon flux at day 21 was analyzed (n=5). **(C)** Image of resected xenografts of nude mice injected intrahepatically with Sorafenib-resistant HepG-2 cells. **(D)** Survival of mice from different groups (n=5). **(E)** Representative immunohistochemical staining for GPX4 and DHODH in HCC tissues from different groups (scale bar, 25 μ m). **(B)** The data are shown as the means \pm S.E.M. ANOVA with Dunnett's *t*-test. **(D)** Log-rank test. ****p* < 0.001.

proteins can efficiently sort miRNAs and other RNAs into exosomes *via* protein-RNA interactions (30, 31). In light of these data, we hypothesized that fusion of an exosomal membrane protein with a specific RNA-binding protein would increase the loading efficiency of the siRNA of interest; therefore, we fused the RNA recognition motif of U1-A with the C-terminus of Lamp2b, which interacts with the sequence “AUUGCAC” in the target RNA with a relatively high affinity. Then, a multi-siRNA

was engineered to harbor the consensus “AUUGCAC” sequence. The preliminary data here indicate that the fusion protein helps sort multiple siRNAs containing the “AUUGCAC” sequence into exosomes during exosome biogenesis, especially when the RNA of interest is exogenously overexpressed. It is worth noting that due to the limitation of the present siRNA detection technology, the biological loading rate of multi-siRNA cannot be accurately detected in live cells and exosomes. Here, in the preparation of



functionalized exosomes, saturated amount of multi-siRNAs were transfected into cells to ensure that engineered exosomes were loaded with sufficient multi-siRNAs. Further experiments also confirmed that a large amount of multi-siRNAs could be effectively encapsulated into engineered exosomes and delivered to HCC cells, thus inducing down-regulation of GPX4 and DHODH. Our study established a novel strategy to efficiently load therapeutic multi-siRNA cargos into exosomes.

Currently, the poor solubility and potential off-target toxicity to normal cells and tissues preclude the systematic use of traditional ferroptosis inducers *in vivo* (32–34). Nanoscale exosomes are considered a good choice as a drug vehicle because exosomes could be engineered toward better targeting specificity *via* exosome surface protein modifications (35–39). For example, exosomes expressing the $\alpha\gamma$ integrin-specific iRGD peptide fused to LAMP-2b efficiently delivered doxorubicin to integrin-positive breast cancer cells *in vitro* and *in vivo* (40). Here, an HCC-specific targeting peptide, SP94, was fused to the extracellular domain of LAMP-2B at the N-terminus (21). Our data show that functionalized exosomes (Exo^{SP94-lamp2b-RRM}-multi-siRNA) can selectively deliver therapeutic cargos to human HCC cells with no obvious adverse effects. This is the first report of tumor-targeted exosome delivery of ferroptosis inducers, which might open a new avenue for the systematic use of ferroptosis inducers to treat cancer.

In summary, this study firstly identified that ferroptosis suppressor genes GPX4 and DHODH were enriched in sorafenib-resistant HCC and associated with compromised therapeutic efficiency of sorafenib. In addition, we described the use of multi-siRNA to enhance sorafenib-induced ferroptosis

by simultaneously knocking down GPX4 and DHODH. More importantly, we designed HCC-targeted engineered exosomes (Exo^{SP94-Lamp2b-RRM}) to deliver multi-siRNA, thus overcoming acquired resistance to sorafenib from the perspective of ferroptosis.

DATA AVAILABILITY STATEMENT

The datasets presented in this study can be found in online repositories. The names of the repository/repositories and accession number(s) can be found in the article/**Supplementary Material**.

ETHICS STATEMENT

The animal study was reviewed and approved by Animal Care and Use Committee of Fourth Military Medical University.

AUTHOR CONTRIBUTIONS

XL, QY, and RZ contributed equally to this work. YG, CZ, and YZ contributed to project conceptualization and supervision. YG, XL, QY, CL, XG, RZ, and KZ contributed to the investigation. WQZ, SW, QH, WL, and ML contributed to the data curation; YG and XL contributed to writing the original draft; YG, CZ, YZ, WZ, and XL contributed to writing, reviewing, and editing the manuscript; and

YG, CZ, and SW contributed to funding acquisition. All authors contributed to the article and approved the submitted version.

FUNDING

This work was financially supported by grants from the Hong Kong Scholar Program; the National Natural Science Foundation of China (NSFC), NO. 81902678, 81802632, 82072910; the Key Research and Development Program of Shaanxi Province (NO. 2017ZDCXL-SF-01-03); and the Young Elite Scientist Sponsorship Program by CAST (No. YESS20210177).

REFERENCES

- Siegel RL, Miller KD, Jemal A. Cancer Statistics, 2018. *CA Cancer J Clin* (2018) 68:7–30. doi: 10.3322/caac.21442
- Bray F, Ferlay J, Soerjomataram I, Siegel RL, Torre LA, Jemal A. Global Cancer Statistics 2018: GLOBOCAN Estimates of Incidence and Mortality Worldwide for 36 Cancers in 185 Countries. *CA Cancer J Clin* (2018) 68:394–424. doi: 10.3322/caac.21492
- Yang JD, Hainaut P, Gores GJ, Amadou A, Plymoth A, Roberts LR. A Global View of Hepatocellular Carcinoma: Trends, Risk, Prevention and Management. *Nat Rev Gastroenterol Hepatol* (2019) 16:589–604. doi: 10.1038/s41575-019-0186-y
- Cheng AL, Kang YK, Chen Z, Tsao CJ, Qin S, Kim JS, et al. Efficacy and Safety of Sorafenib in Patients in the Asia-Pacific Region With Advanced Hepatocellular Carcinoma: A Phase III Randomised, Double-Blind, Placebo-Controlled Trial. *Lancet Oncol* (2009) 10:25–34. doi: 10.1016/S1470-2045(08)70285-7
- Chen X, Kang R, Kroemer G, Tang D. Broadening Horizons: The Role of Ferroptosis in Cancer. *Nat Rev Clin Oncol* (2021) 18:280–96. doi: 10.1038/s41571-020-00462-0
- Wang Q, Bin C, Xue Q, Gao Q, Huang A, Wang K, et al. GSTZ1 Sensitizes Hepatocellular Carcinoma Cells to Sorafenib-Induced Ferroptosis via Inhibition of NRF2/GPX4 Axis. *Cell Death Dis* (2021) 12:426. doi: 10.1038/s41419-021-03718-4
- Su Y, Zhao B, Zhou L, Zhang Z, Shen Y, Lv H, et al. Ferroptosis, a Novel Pharmacological Mechanism of Anti-Cancer Drugs. *Cancer Lett* (2020) 483:127–36. doi: 10.1016/j.canlet.2020.02.015
- Sun X, Ou Z, Chen R, Niu X, Chen D, Kang R, et al. Activation of the P62-Keap1-NRF2 Pathway Protects Against Ferroptosis in Hepatocellular Carcinoma Cells. *Hepatology* (2016) 63:173–84. doi: 10.1002/hep.28251
- Lachaier E, Louandre C, Godin C, Saidak Z, Baert M, Diouf M, et al. Sorafenib Induces Ferroptosis in Human Cancer Cell Lines Originating From Different Solid Tumors. *Anticancer Res* (2014) 34:6417–22.
- Dixon SJ, Patel DN, Welsch M, Skouta R, Lee ED, Hayano M, et al. Pharmacological Inhibition of Cystine-Glutamate Exchange Induces Endoplasmic Reticulum Stress and Ferroptosis. *Elife* (2014) 3:e2523. doi: 10.7554/eLife.02523
- Coriat R, Nicco C, Chereau C, Mir O, Alexandre J, Ropert S, et al. Sorafenib-Induced Hepatocellular Carcinoma Cell Death Depends on Reactive Oxygen Species Production *In Vitro* and *In Vivo*. *Mol Cancer Ther* (2012) 11:2284–93. doi: 10.1158/1535-7163.MCT-12-0093
- Dietrich P, Koch A, Fritz V, Hartmann A, Bosserhoff AK, Hellerbrand C. Wild Type Kirsten Rat Sarcoma is a Novel microRNA-622-Regulated Therapeutic Target for Hepatocellular Carcinoma and Contributes to Sorafenib Resistance. *Gut* (2018) 67:1328–41. doi: 10.1136/gutjnl-2017-315402
- Gao Y, Wang Z, Hao Q, Li W, Xu Y, Zhang J, et al. Loss of ERalpha Induces Amoeboid-Like Migration of Breast Cancer Cells by Downregulating Vinculin. *Nat Commun* (2017) 8:14483. doi: 10.1038/ncomms14483
- Dixon SJ, Stockwell BR. The Role of Iron and Reactive Oxygen Species in Cell Death. *Nat Chem Biol* (2014) 10:9–17. doi: 10.1038/nchembio.1416
- Seibt TM, Proneth B, Conrad M. Role of GPX4 in Ferroptosis and its Pharmacological Implication. *Free Radic Biol Med* (2019) 133:144–52. doi: 10.1016/j.freeradbiomed.2018.09.014

ACKNOWLEDGMENTS

We thank Ms. Wang Wei for drawing the Graphical Abstract.

SUPPLEMENTARY MATERIAL

The Supplementary Material for this article can be found online at: <https://www.frontiersin.org/articles/10.3389/fonc.2022.898156/full#supplementary-material>

- Feng H, Stockwell BR. Unsolved Mysteries: How Does Lipid Peroxidation Cause Ferroptosis? *PLoS Biol* (2018) 16:e2006203. doi: 10.1371/journal.pbio.2006203
- Wang F, Min J. DHODH Tangoing With GPX4 on the Ferroptotic Stage. *Signal Transduct Target Ther* (2021) 6:244. doi: 10.1038/s41392-021-00656-7
- Herrmann IK, Wood M, Fuhrmann G. Extracellular Vesicles as a Next-Generation Drug Delivery Platform. *Nat Nanotechnol* (2021) 16:748–59. doi: 10.1038/s41565-021-00931-2
- Wang F, Adams A, King KE, Dunn W, Christenson LK, Hung WT, et al. The RNA Binding Protein FMR1 Controls Selective Exosomal miRNA Cargo Loading During Inflammation. *J Cell Biol* (2020) 219:e201912074. doi: 10.1083/jcb.201912074
- Bolduc F, Turcotte MA, Perreault JP. The Small Nuclear Ribonucleoprotein Polypeptide a (SNRPA) Binds to the G-Quadruplex of the BAG-1 5'utr. *Biochimie* (2020) 176:122–7. doi: 10.1016/j.biochi.2020.06.013
- Zhou T, Liang X, Wang P, Hu Y, Qi Y, Jin Y, et al. A Hepatocellular Carcinoma Targeting Nanostrategy With Hypoxia-Ameliorating and Photothermal Abilities That, Combined With Immunotherapy, Inhibits Metastasis and Recurrence. *ACS Nano* (2020) 14:12679–96. doi: 10.1021/acsnano.0c01453
- Garcia-Bermudez J, Birsoy K. A Mitochondrial Gatekeeper That Helps Cells Escape Death by Ferroptosis. *Nature* (2021) 593:514–5. doi: 10.1038/d41586-021-01203-8
- Stockwell BR, Friedmann AJ, Bayir H, Bush AI, Conrad M, Dixon SJ, et al. Ferroptosis: A Regulated Cell Death Nexus Linking Metabolism, Redox Biology, and Disease. *Cell* (2017) 171:273–85. doi: 10.1016/j.cell.2017.09.021
- Zhang Y, Shi J, Liu X, Feng L, Gong Z, Koppula P, et al. BAP1 Links Metabolic Regulation of Ferroptosis to Tumour Suppression. *Nat Cell Biol* (2018) 20:1181–92. doi: 10.1038/s41556-018-0178-0
- Mao C, Liu X, Zhang Y, Lei G, Yan Y, Lee H, et al. DHODH-Mediated Ferroptosis Defence is a Targetable Vulnerability in Cancer. *Nature* (2021) 593:586–90. doi: 10.1038/s41586-021-03539-7
- Fu Z, Zhang X, Zhou X, Ur-Rehman U, Yu M, Liang H, et al. *In Vivo* Self-Assembled Small RNAs as a New Generation of RNAi Therapeutics. *Cell Res* (2021) 31:631–48. doi: 10.1038/s41422-021-00491-z
- van Niel G, D'Angelo G, Raposo G. Shedding Light on the Cell Biology of Extracellular Vesicles. *Nat Rev Mol Cell Biol* (2018) 19:213–28. doi: 10.1038/nrm.2017.125
- Ohno S, Takanashi M, Sudo K, Ueda S, Ishikawa A, Matsuyama N, et al. Systemically Injected Exosomes Targeted to EGFR Deliver Antitumor microRNA to Breast Cancer Cells. *Mol Ther* (2013) 21:185–91. doi: 10.1038/mt.2012.180
- Kooijmans S, Stremersch S, Braeckmans K, de Smedt SC, Hendrix A, Wood M, et al. Electroporation-Induced siRNA Precipitation Obscures the Efficiency of siRNA Loading Into Extracellular Vesicles. *J Control Release* (2013) 172:229–38. doi: 10.1016/j.jconrel.2013.08.014
- Gao Y, Li X, Zeng C, Liu C, Hao Q, Li W, et al. CD63(+) Cancer-Associated Fibroblasts Confer Tamoxifen Resistance to Breast Cancer Cells Through Exosomal miR-22. *Adv Sci (Weinh)*. (2020) 7:2002518. doi: 10.1002/advs.202002518
- Zhang H, Deng T, Liu R, Ning T, Yang H, Liu D, et al. CAF Secreted miR-522 Suppresses Ferroptosis and Promotes Acquired Chemo-Resistance in Gastric Cancer. *Mol Cancer* (2020) 19:43. doi: 10.1186/s12943-020-01168-8

32. Yu M, Gai C, Li Z, Ding D, Zheng J, Zhang W, et al. Targeted Exosome-Encapsulated Erastin Induced Ferroptosis in Triple Negative Breast Cancer Cells. *Cancer Sci* (2019) 110:3173–82. doi: 10.1111/cas.14181
33. Lu B, Chen XB, Ying MD, He QJ, Cao J, Yang B. The Role of Ferroptosis in Cancer Development and Treatment Response. *Front Pharmacol* (2017) 8:992. doi: 10.3389/fphar.2017.00992
34. Stockwell BR, Jiang X. The Chemistry and Biology of Ferroptosis. *Cell Chem Biol* (2020) 27:365–75. doi: 10.1016/j.chembiol.2020.03.013
35. Yi J, Minikes AM, Jiang X. Aiming at Cancer *In Vivo*: Ferroptosis-Inducer Delivered by Nanoparticles. *Cell Chem Biol* (2019) 26:621–2. doi: 10.1016/j.chembiol.2019.05.002
36. Terasawa K, Tomabechi Y, Ikeda M, Ehara H, Kukimoto-Niino M, Wakiyama M, et al. Lysosome-Associated Membrane Proteins-1 and -2 (LAMP-1 and LAMP-2) Assemble via Distinct Modes. *Biochem Biophys Res Commun* (2016) 479:489–95. doi: 10.1016/j.bbrc.2016.09.093
37. Armstrong JP, Holme MN, Stevens MM. Re-Engineering Extracellular Vesicles as Smart Nanoscale Therapeutics. *ACS Nano* (2017) 11:69–83. doi: 10.1021/acsnano.6b07607
38. Yang J, Wu S, Hou L, Zhu D, Yin S, Yang G, et al. Therapeutic Effects of Simultaneous Delivery of Nerve Growth Factor mRNA and Protein via Exosomes on Cerebral Ischemia. *Mol Ther Nucleic Acids* (2020) 21:512–22. doi: 10.1016/j.omtn.2020.06.013
39. Kim H, Yun N, Mun D, Kang JY, Lee SH, Park H, et al. Cardiac-Specific Delivery by Cardiac Tissue-Targeting Peptide-Expressing Exosomes. *Biochem Biophys Res Commun* (2018) 499:803–8. doi: 10.1016/j.bbrc.2018.03.227
40. Tian Y, Li S, Song J, Ji T, Zhu M, Anderson GJ, et al. A Doxorubicin Delivery Platform Using Engineered Natural Membrane Vesicle Exosomes for Targeted Tumor Therapy. *Biomaterials* (2014) 35:2383–90. doi: 10.1016/j.biomaterials.2013.11.083

Conflict of Interest: The authors declare that the research was conducted in the absence of any commercial or financial relationships that could be construed as a potential conflict of interest.

Publisher's Note: All claims expressed in this article are solely those of the authors and do not necessarily represent those of their affiliated organizations, or those of the publisher, the editors and the reviewers. Any product that may be evaluated in this article, or claim that may be made by its manufacturer, is not guaranteed or endorsed by the publisher.

Copyright © 2022 Li, Yu, Zhao, Guo, Liu, Zhang, Zhang, Liu, Yu, Wang, Hao, Li, Zhang, Li, Zhang, Zhang and Gao. This is an open-access article distributed under the terms of the Creative Commons Attribution License (CC BY). The use, distribution or reproduction in other forums is permitted, provided the original author(s) and the copyright owner(s) are credited and that the original publication in this journal is cited, in accordance with accepted academic practice. No use, distribution or reproduction is permitted which does not comply with these terms.